Synthetic Metals 175 (2013) 21–29

Contents lists available at SciVerse ScienceDirect

Synthetic Metals

journal homepage: www.elsevier.com/locate/synmet

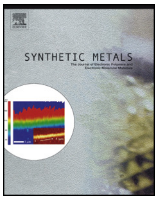

Novel conjugated polymers with planar backbone bearing acenaphtho[1,2-*b*]quinoxaline acceptor subunit for polymer solar cells

Zhanyuan Zhang[a], Qing Peng[b], Daobin Yang[a], Yunqing Chen[a], Yan Huang[a,*], Xuemei Pu[a], Zhiyun Lu[a,*], Qing Jiang[a], Yu Liu[b,*]

[a] College of Chemistry, Sichuan University, Chengdu, 610064, People's Republic of China
[b] Key Laboratory of Environmentally Friendly Chemistry and Applications of Ministry of Education, College of Chemistry, Xiangtan University, Hunan 411105, People's Republic of China

ARTICLE INFO

Article history:
Received 18 January 2013
Received in revised form 16 April 2013
Accepted 18 April 2013
Available online 28 May 2013

Keywords:
Conjugated polymers
PSCs
Donor-acceptor
Bulk heterojunction
Phase separation

ABSTRACT

Dialkoxy substituted acenaphtho [1,2-*b*]quinoxaline (AQx) is demonstrated to be a promising electronic acceptor subunit for constructing high performance donor-acceptor (D–A) photovoltaic copolymers. Using it as acceptor and benzo[1,2-*b*:4,5-*b*′]-dithiophene (BDT) or thiophene (T) as donor units, two D–A conjugated polymers (abbr. as **PB** and **PT** respectively) are synthesized via Stille coupling reaction. The incorporation of alkoxy groups with quinoxaline moiety is found to be beneficial to both the enhanced solubility and the maintained coplanarity of the backbone due to strong S···O attractive interaction. UV–vis absorption and XRD characterization results indicate that the presence of planar AQx moiety could lead to well-ordered packing in solid state, and **PB** bearing planar BDT electron-donating subunit exhibits more intensified molecular self-organization. Both **PB** and **PT** possess deep HOMO energy level of −5.4∼−5.5 eV, and **PB**-based photovoltaic devices show maximum PCE value of 1.20% (V_{oc} = 0.78 V, J_{sc} = 3.58 mA cm^{-2}, FF = 0.43) under air mass 1.5 global (AM 1.5 G) irradiation of 100 mW cm^{-2}.

1. Introduction

As the next generation of renewable energy technology, polymer solar cells (PSCs) have attracted considerable attention due to their technological potential for low cost, light weight, flexible and large area photovoltaic application by facile ink-jet or roll-to-roll solution processes [1–6]. Among the various device structures, bulk heterojunction (BHJ) that comprise interpenetrating networks of electron-donating conjugated polymers and electron-accepting fullerene derivatives (PCBMs) has been demonstrated to be the most successful one [3–8], and the power conversion efficiency (PCE) of BHJ PSCs, thanks to the enthusiastic efforts of scientists, has been enhanced to >8% over the past 10 years [9–11]. Nevertheless, the exploitation of p-type polymers with appropriate absorption bands, HOMO (highest occupied molecular orbital) and LUMO (lowest unoccupied molecular orbital) energy levels, and carrier mobility continues to dominate this research area for achieving high performance devices, and the most promising candidates are conjugated in-chain D–A copolymers with alternating donor and acceptor segments in each repeating unit [12–14]. Yet compared to the well-developed D building blocks, effective acceptor subunits are still limited in quantity, although the incorporation of appropriate A moiety with D segments is a crucial factor for constructing high performance D–A polymers [15].

Recently, there have been some research efforts constructing D–A copolymer using electron-deficient planar fused aromatic system as A subunit, so that better π–π stacking between the polymeric chains and strong absorption could be realized simultaneously, accordingly high charge carrier transport capability could be achieved [16–25]. For example, the macromolecule ACTP-F with acenaphtho[1,2-*b*]thieno[3,4-*e*]pyrazine (ACTP) as A and fluorene as D moieties is found to show high charge mobility of 0.2 cm^2 V^{-1} s^{-1} [16], which is extremely beneficial to the performance of PSCs. Nevertheless, the PCE of ACTP-F-based PSCs are not quite satisfied, which might partially be ascribed to their relatively low open circuit voltage (V_{oc}) stemming from the relatively high HOMO (∼−5.0 eV) of ACTP-F[17]. As deeper HOMO energy level of the donor material is propitious to the maximization of V_{oc} [26–28], recently, by replacing thienopyrazine with quinoxaline segment, we developed a new planar A building block, namely, dithiophenyl-substituted acenaphtho[1,2-*b*]quinoxaline (DTAQx), which is more electron-deficient relative to ACTP. Using it as A subunit, a series of D–A copolymers with lower lying HOMO levels of ∼−5.5 eV have been synthesized, and PSCs based on them show maximum V_{oc} of 0.84 V. However, the PCEs of these devices are still relatively low

---

* Corresponding authors. Tel.: +86 28 85410059.
E-mail addresses: huangyan@scu.edu.cn (Y. Huang), luzhiyun@scu.edu.cn (Z. Lu), liuyu03b@126.com (Y. Liu).

0379-6779/$ – see front matter © 2013 Elsevier B.V. All rights reserved.
http://dx.doi.org/10.1016/j.synthmet.2013.04.024

(<0.9%), this might be ascribed to the low molecular weights due to the poor solubility of the polymers [29], which are adverse factors for the control of film morphology and processing conditions [30]. Although by introducing long side-chains into the conjugated backbone, the solubility of polymeric materials might be improved, the incorporation of electron-donating alkyls or alkyloxys with D subunits would generally lead to elevated HOMO energy levels. In addition, the substituents might also bring substantial effect on the torsional angles between the aromatic moieties in the backbone, consequently lead to much differed intermolecular ordering and charge-carrier transporting across the polymer stacks [31,32]. Therefore, the substituent species and substitutive position are both essential factors determining the photovoltaic properties of the polymers. As HOMO levels are generally dominated by the donor segment of D–A copolymers, herein, we introduce side-chains into the DTAQx acceptor subunit to maintain the deep HOMOs of the parent polymers, while alkyloxy rather than alkyl substituents are directed into quinoxaline moiety, since according to density functional theory (DFT) computation results, if alkyloxy groups are attached to the quinoxaline moiety, the intramolecular S···O attractive interaction [33,34] between thienyl and alkoxyl units might help the DTAQx moiety keep a coplanar structure. Our results indicate that in comparison with their parent polymers, the dialkyloxy-substituted objective macromolecules possess much higher molecular weights, and PSCs based on them show improved PCE.

2. Experimental

2.1. Materials and instrument

All the chemicals were purchased from commercial suppliers and used without further purification. Tetrahydrofuran (THF) and toluene were freshly distilled over sodium/benzophenone ketyl under nitrogen before use. Electron-accepting fullerene derivative (PCBM) used in the fabrication of photovoltaic cells are all $PC_{61}BM$. ^1H NMR and ^{13}C NMR spectra were recorded on a Bruker AV II-400 MHz spectrometer using tetramethylsilane as an internal standard. High resolution MS spectra were obtained from a Q-TOF Priemier ESI mass spectrometer (Micromass, Manchester, UK). UV–vis absorption spectra of the polymers in 10^{-6} mol L^{-1} chlorobenzene (CB) solutions and thin films casted from CB solution (10 mg mL^{-1}) at 1500 rpm on quartz substrates were recorded on a Shimadzu UV2100 UV–vis spectrophotometer. Number-average (M_n) and weight-average (M_w) molecular weights and polydispersity indices (PDI) of the polymers were determined on a PL-GPC model 210 chromatograph at 25 °C at a flow rate of 1 mL min^{-1}, and the calibration was based on polystyrene standards. Thermogravimetric analysis (TGA) was performed on a Perkin-Elmer TGA-7 under nitrogen atmosphere at a heating rate of 10 °C min^{-1}. Electrochemical measurements were conducted on a PARSTAT electrochemical workstation at a scan rate of 100 mV s^{-1} using tetrabutylammonium perchlorate (0.1 mol L^{-1}) as supporting electrolyte in acetonitrile. Polymer-precoated platinum electrode, platinum-wire electrode, and Ag/Ag^+ electrode were used as working electrode, anauxiliary electrode, and reference electrode, respectively. Each measurement was calibrated using a ferrocene/ferrocenium (Fc/Fc^+) redox couple as internal standard. X-ray diffraction (XRD) data were generated using the Philips DX-100 sealed-tube X-ray generator (Cu target; $I = 0.2$ nm) with power of 40 kV and 35 mA, and the scanning angle was every 0.2° step over the range of 2–30°. The morphologies of the active layers were investigated through atomic force microscopy (AFM) in tapping mode under ambient conditions using a MFP 3D Asylum Research instrument.

2.2. Fabrication and characterization of polymer solar cells

The photovoltaic cells were fabricated with a traditional sandwich structure through the following steps. The ITO coated glass substrates were cleaned by a series of ultrasonic treatments for 10 min in acetone, following by deionized water and then 2-propanol. The substrates were dried under a nitrogen stream and subjected to the treatment of Ar/O_2 plasma for 5 min. A filtered aqueous solution of poly(3,4-ethylenedioxythiophene): poly(styrenesulfonate) (PEDOT:PSS; Bayer AG, 4083) was spin-coated onto the ITO surface at 2000 rpm for 30 s and then thermal treated at 150 °C for 30 min to form a PEDOT:PSS thin film with a thickness of 30 nm. A blend of copolymer and $PC_{61}BM$ was dissolved in chlorobenzene (25 mg mL^{-1}), filtered through a 0.45 μm poly(tetrafluoroethylene) filter and spin-coated at 1500 rpm for 30 s onto the PEDOT:PSS layer. Then the substrates were dried under N_2 at room temperature or annealed at 120 °C for 10 min in a nitrogen-filled glovebox. The devices were completed after thermal deposition of 0.75 nm lithium fluoride and 100 nm aluminum as the cathode at a pressure of 6×10^{-4} Pa. The active area was 9 mm^2 for each cell. The thicknesses of the spin-casted films were recorded by a profilometer (Alpha-Step 200; Tencor Instruments). Device characterization was carried out under an AM 1.5 G irradiation with an intensity of 100 mW cm^{-2} (Oriel 91160, 300 W) calibrated by a NREL-certified standard silicon cell. Current density–voltage (*J–V*) characteristics were measured by a computer-controlled Keithley 2602 source measurement unit in the dark. All device characterizations were performed in an ambient atmosphere at room temperature.

2.3. Synthesis of the monomers and polymers

The synthetic routes to the monomers and polymers are shown in Scheme 1 and Scheme 2. The detailed synthetic processes are as follows. $Pd(PPh_3)_4$ [35], 1,2-dioctyloxybenzene (1) [36], 1,2-dinitro-4,5-dioctyloxybenzene (2) [36], 5,6-dioctyloxybenzo[1,2,5]thiadiazole (3) [36], 4,7-dibromo-5,6-dioctyloxybenzo[1,2,5]thiadiazole (4) [36], were synthesized according to the literature procedures, 2,5-bis-(tributylstannyl)thiophene (T-Sn) and 2,6-bis(trimethylstannyl)-4,8-di(2-ethylhexyloxy)benzo[1,2-b;4,5-b′]dithiophene (BDP-Sn) were purchased and recrystallized from isopropanol before polymerization reaction [37,38].

2.3.1. Synthesis of 8,11-dibromo-9,10-dioctyloxyacenaphtho-[1,2-b]quinoxaline (**5**)

To a suspension of compound **4** (5.5 g, 10 mmol) in EtOH (100 mL) was added $NaBH_4$ (3.8 g, 100 mmol) portionwise at 0 °C, followed by stirring overnight at room temperature. After the removal of solvent in *vacuo*, 100 mL of water was added, and the mixture was filtered, washed with water (30 mL) and dried under vacuum to afford white solid (2.6 g, 5.00 mmol). This white solid was dissolved in mixture of acetic acid (20 mL) and acetonitrile (20 mL), then acenaphthequinone (0.91 g, 5.00 mmol) was added portionwise under stirring, followed by refluxing for 6 h under N_2. After cooled down, the pale yellow solid precipitated was filtered off, washed with water, and recrystallized from EtOH to afford white crystal (2.54 g, yield: 38%). ^1H NMR (400 MHz, $CDCl_3$,): δ (ppm) 8.52 (d, $J = 7.2$ Hz, 2H); 8.13 (d, $J = 8$ Hz, 2H); 7.85 (t, $J = 7.6$ Hz, 2H); 4.23–4.21 (m, 4H); 1.99–1.92 (t, $J = 7.2$ Hz, 4H); 1.57–1.32 (m, 20H); 0.91–0.89 (m, 6H). ^{13}C NMR (100 MHz, $CDCl_3$): δ (ppm) 153.82, 152.91, 137.58, 136.50, 131.20, 129.88, 129.83, 128.58, 122.85, 118.53, 74.80, 31.88, 30.35, 29.48, 29.32, 26.10, 22.69, 14.11. TOF-MS: m/z: 689.1354 ($M+Na^+$); Calcd for M_w+Na^+: 689.4512.